Cell-to-cell scaling approach to the dielectric breakdown model

1991 J. Phys. A: Math. Gen. 24 1281

(http://iopscience.iop.org/0305-4470/24/6/020)

J. Phys. A: Math. Gen. 24 (1991) 1281–1291. Printed in the UK

Cell-to-cell scaling approach to the dielectric breakdown model

R Dekeyser†, A Maritan‡|| and A Stella§¶

† Instituut voor Theoretische Fysica, Katholieke Universiteit Leuven, B-3001 Leuven, Belgium

‡ Dipartimento de Fisica dell'Università degli Studi di Bari and INFN, Sezione di Bari, I-70126 Bari, Italy

§ Dipartimento di Fisica Università di Bologna, I-47126 Bologna, Italy, and Centro Interuniversitario di Struttura della Materia di Padova, I-35131 Padova, Italy

Received 25 September, in final form 19 December 1990

Abstract. A new ansatz is proposed to implement finite size scaling analysis of the dielectric breakdown model. Calculations on very small cells already allow to obtain good qualitative determinations of the fractal dimensions $\bar{d}$ in a wide range of dimensionalities and model parameters. Exact enumerations or high accuracy Monte Carlo calculations on larger cells ($\leqslant 12\times 12$) in $d=2$ show a remarkable degree of convergence towards values known from large scale simulations for $\bar{d}$, and, to a lesser extent, for the multifractal dimension $D(q)$ with $q \geqslant -1$. General difficulties inherent to Monte Carlo determinations of $D(q)$ for negative q are also pointed out. For calculating the electrostatic potential inside these cells we use a new exact and fast algorithm, explained in detail in the appendix.

1. Introduction

Dielectric breakdown [1] (DBM) and diffusion limited aggregation [2] (DLA) are among the most extensively studied models of fractal growth. In spite of many efforts, up to now these models could be treated mostly numerically [3]. From a more theoretical point of view, there have of course been several attempts to develop analytical approaches to these problems. Among them the most close in spirit to the method we present here, are certainly those of the real space renormalization group (RSRG) type [4–9]. In addition we should also mention the rather promising approach by Pietronero *et al* [10] based on a fixed scale transformation. This last method, however, is only implicitly based on scale invariance and relies essentially on another invariance principle, so that it should not be regarded as belonging to the RSRG category.

The general problem with RSRG approaches is that they are often rather qualitative, and do not allow systematic improvement, being based on uncontrollable approximations. That is the reason why, very often, one has to rely on more quantitative scaling approaches, like phenomenological renormalization [11], when an accurate determination of scaling properties is needed.

When trying to apply similar strategies to fractal growth problems like DBM, one meets further serious difficulties. The real goal of an RSRG approach in this case would be to map the growth rules at a given scale into new rules at a coarse grained scale.

|| Also at Instituto Nazionale di Fisica Nucleare, Sezione di Padova, Italy.

¶ Also at International School for Advanced Studies, I-34014 Trieste, Italy, and Unitá di Padova, Gruppo Nazionale di Struttura della Materia del Consiglio Nazionale delle Ricerche, Padova, Italy.

0305-4470/91/061281+11$03.50

By imposing a fixed point condition for the mapping, consistent with the fact that the grown cluster is fractal, one should then be able to determine its fractal dimension. This strategy is in principle very ambitious. In practice the very choice of the parameters which should determine the growth rules (the type and degree of proliferation, in RG language) appears rather arbitrary, and it does not seem possible to go beyond a rather qualitative level with similar calculations [4, 6, 8, 9].

In the present work a serious effort is made in order to optimally exploit finite size scaling (FSS) ideas in the study of the DBM and similar models. Like in the case of phenomenological renormalization for, e.g., equilibrium spin problems, our FSS based strategy does not meet the difficulty of handling proliferation and has the big advantage of allowing, at least in principle, a clear way of systematic improvement of the results, i.e. that of increasing the sizes involved in the actual calculations. Below, we make a first attempt along this way, and show at the same time how to extract meaningful qualitative results also from calculations on systems of very small size.

2. Finite size scaling on small cells

A standard formulation of FSS for a model like the DBM is as follows. Consider a finite (e.g., square in $d=2$) region of size L in the space where cluster growth occurs. Indicating by $N(L, t)$ the total number of cluster sites within the box at time t, we expect the following type of homogeneity, for big L and t:

$$N(L, t) = l^{\bar{d}} N\left(\frac{L}{l}, \frac{t}{l^z}\right) \tag{2.1}$$

with $z = \bar{d}$, the fractal dimension of the cluster. Indeed, we must have that $N(\infty, t) = l^{\bar{d}} N(\infty, t/l^z)$ but, of course, $N(\infty, t) = t$. In this framework one imagines that the growth actually occurs in a space region much bigger than the box of side L. The trouble with (2.1) is that it cannot be easily implemented because, e.g., growth has to proceed on space (and time) scales much larger than L before the cluster freezes as a consequence of screening. Here we substitute (2.1) with another scaling ansatz, which avoids these difficulties and is directly inspired by the actual situation realized in dielectric breakdown experiments.

Suppose that the perimeter of our box of side L corresponds to the external electrode and that growth starts from a point electrode in the middle of the box. In this case growth will have to stop at the time by which the first branch of the cluster hits the boundary. Indicating by $N(L)$ the average number of sites of the cluster at this short-circuiting situation, we expect that $N(L)$ should scale simply as $L^{\bar{d}}$, for large L. In other words, the scaling occurring in the previous situation for $t \to \infty$ and large L should reveal the same fractal dimension as the scaling just defined. The advantage is that in the latter case we can hope to get meaningful results by restricting the global growths completely within the limits of our cells.

Unless otherwise specified, we will consider here the DBM growth [1] within cells whose boundary is kept at a fixed potential, say $\Phi = 1$. An interior point, playing the role of seed for cluster growth, is kept at $\Phi = 0$ from the start. For points not belonging to the cluster, the potential satisfies the discrete Laplace equation, while for those of the cluster $\Phi = 0$. At each stage of growth one bond is chosen among those on the perimeter of the cluster with probability proportional to $\Delta\Phi_b^{\eta}$, where $\Delta\Phi_b$ is the potential drop across the boundary of the cluster, and η is a parameter of the model.

The average number of points in the cluster, N, is obtained by summing the number of cluster sites of each possible growth pattern at the moment of breakdown, multiplied by the probability of that pattern.

For relatively small cells such a calculation soon becomes a formidable task, and one needs to perform it on the computer, either exactly or by some Monte Carlo procedure, as we will discuss below.

The smallest conceivable cells with which we can try to implement our scaling ansatz are the one- and two-site cells. For both the calculation of N is still extremely simple. For the first, since the seed point coincides with the unique cell site, and the boundary sites are its $2d$ nearest neighbours, breakdown occurs at the first step of growth, and trivially $N(1)=1$. The two-site cell can also be worked out, with one of the two sites playing the role of seed, and with the $2(2d-1)$ surrounding sites playing the role of boundary. The seed site is surrounded by $2d-1$ boundary sites (with a potential difference equal to unity) and by the second interior site, with a potential $\Phi_0=(2d-1)/2d$ (the average of the potentials of its neighbours). If dielectric breakdown occurs by an immediate growth from the seed to the boundary, we count a single site in the final cluster. Only if the initial growth goes to the second site (which happens with relative probability Φ_0^η), we end up with two sites. In this way we get

$$N(2)=\frac{2d-1+2\Phi_0^\eta}{2d-1+\Phi_0^\eta}. \tag{2.2}$$

It is remarkable that we can obtain already from the above elementary calculations a qualitative description of the properties of DBM. Due to the extreme smallness of our cells, a meaningful definition of the rescaling factor l between them is not possible. Some ambiguity in the definition of l is always affecting very small and asymmetric cell calculations. Instead of using a standard $l=2^{1/d}$, we profit from the ambiguity with an *ad hoc* definition of l. The rescaling can be chosen such that the fractal dimension $\bar{d}$ provided by our scaling exactly coincides with d for $\eta=0$, as we know to be the case (Eden model) [12]. We finally get

$$\bar{d}=d\ln\left(\frac{2d-1+2(1-1/2d)^\eta}{2d-1+(1-1/2d)^\eta}\right)\left[\ln\left(1+\frac{1}{2d}\right)\right]^{-1}. \tag{2.3}$$

This is an interesting formula, because it includes both d- and η-dependences. As a function of d, for $\eta=1$, e.g., the agreement of this formula with existing estimates is rather satisfactory. For $d=2,3,\ldots,6$ we get $\bar{d}=1.63, 2.60, 3.58, 4.57,\ldots$ respectively, to be compared with the corresponding estimates 1.70, 2.51, 3.34, 4.20, 5.3 ... [3]. As a function of η, at fixed d, the behaviour is also satisfactory for η not too large. For $\eta\to\infty$ we do not recover $\bar{d}\to 1$, because the geometry of the cluster and the choice of the starting point do not allow this. Nevertheless, for $d=2$, e.g., we get $\bar{d}=1.812$ and 1.314 for $\eta=0.5$ and 2 respectively. These values should be compared with the corresponding Monte Carlo estimates $\bar{d}=1.9$ and 1.4 respectively [3]. At fixed η we get from (2.3) for $d\to\infty$:

$$\bar{d}=d\left(1-\frac{\eta}{2d}\right)+O\left(\frac{1}{d}\right). \tag{2.4}$$

It should be noted that for $\eta=1$ (DLA) this formula satisfies the exact bound $\bar{d}>d-1$ [13].

We believe that the result (2.3) is interesting in at least two respects. On one side it compares well with similar approximations obtained on a basis different from RG [14, 15]. On the other hand it clearly shows that even extremely small scale calculations in this field allow to extract a reasonable qualitative description of the fractal properties.

A more difficult step is that of passing from a qualitative to a more quantitative description, without being compelled to resort to brute, large scale calculations. Within the context of still qualitatively minded approximations we can mention several results obtained along similar lines for clusters with more than two sites in $d=2$ and $d=3$. In these cases one loses the nice possibility of embodying analytically the d-dependence. In table 1 some clusters and the corresponding estimates for $\bar{d}$ are listed. In all these cases the calculations were performed analytically and the *ad hoc* definition of the rescaling described above was adopted.

Table 1. Fractal dimension $\bar{d}$ from some small cell finite size scalings. (Note: for the 2×2-cell, we took an average over all possible starting points.) All results refer to the case $\eta=1$.

Large cell	Small cell	$\bar{d}$ $(d=2)$	$\bar{d}$ $(d=3)$
$2\times2\times1^{d-2}$	$2\times1^{d-1}$	1.59	2.58
3×3	2×2	1.60	

A different possible choice of boundary conditions for the cells are the cylindrical ones. In this case one considers all sites on the bottom of the cell as seed sites and one puts $\Phi=1$ on the sites of the upper boundary. Laterally periodic boundary conditions are used. The result of a four- into a two-site cell rescaling calculation is $\bar{d}=1.76$ for $d=2$ and $\eta=1$. Also in this case, due to the asymmetry of the cells, it is convenient to define l in such a way that the exact result is recovered for $\eta=0$.

3. Calculations on larger cells

In order to extend the calculations of the previous section to larger cells, in the hope of being able to extract results valid asymptotically for very large cells, we can follow several strategies.

The most simple method consists of a straightforward Monte Carlo generation of a large set of DBM realizations in each cell considered, where $N(L)$ is then obtained as an average over this set. The Monte Carlo procedure consists of choosing at each step the next growth site at random between the many candidate sites, with relative probabilities given by their respective values of $\Delta\Phi_p^\eta$.

For cells that are not too large, this Monte Carlo method can be replaced by an exact enumeration of all possible growths up to the breakdown. The enumeration procedure is similar to that used in the enumeration of different kinds of walks on a lattice [16], except for the fact that the number of possibilities at each step is not fixed but determined by the configuration. The value for $N(L)$ is then obtained by averaging N over all configurations at breakdown, with the product of the $\Delta\Phi_p^\eta$ at each step as weight factors.

When the cells become too large to allow an exact enumeration of all possible growth patterns, we have used a combined strategy. We have enumerated all possible

growth patterns consisting of up to N_0 sites (where the maximum acceptable value for N_0 depends on the computational capacity), together with the weight factors of these patterns. If they break down before N_0 is reached, we calculate their contribution to $N(L)$. If the boundary of the cell has not been reached after N_0 steps, we continue from that configuration till breakdown with a Monte Carlo sampling as described above. In order to increase the efficiency of the computation, the number of Monte Carlo runs for each configuration (and thus the accuracy of the estimate) can, e.g., be taken proportional to the weight of the configuration.

Whatever the strategy used, we also need an efficient algorithm to calculate the potentials Φ at the lattice sites for each configuration. Instead of using the standard relaxation method [17], we have developed an exact algorithm, based on the linearity of the problem. In this method a matrix B_{ij} is constructed, containing all the information about a resistor network with sites i and j. Furthermore, each time a new site is added to the growth, this results in linking the two sites with a zero resistance (short circuiting these sites) and this translates into a readjustment of the matrix B through $n(n+1)/2$ simple calculations, where n is the number of sites that have to be monitored. Full details of this method are given in the appendix.

We have applied this method first to square cells with site L, using cylindrical boundary conditions in one direction, and $\Phi=0$ and $\Phi=1$ on the boundaries in the other direction, as already mentioned in the previous section. In these calculations we used $N_0=4$, as we made sure that at least 100 000 Monte Carlo runs were performed for each cell. If we denote by $N(L;\eta)$ the average mass of the growth at breakdown within a square of side L, for a given η we derive estimates for the fractal dimension of the growth $\bar{d}(\eta)$ from

$$\bar{d}(L', L; \eta) = \frac{\ln[N(L;\eta)/N(L';\eta)]}{\ln(L/L')}. \tag{3.1}$$

The results from our simulations are reproduced in table 2, both for $\eta=0$ and $\eta=1$. The values $N(3)$ and $N(4)$ are exact, coming from a complete enumeration. For the other L-values we have estimated the uncertainty on the results by dividing the Monte

Table 2. Values obtained for $N(L;\eta)$, the average mass of the growth at breakdown under cylindrical conditions within a square of side L, for $\eta=0$ and 1, and corresponding estimates for the fractal dimension. Numbers in parentheses indicate uncertainties on last digit. The values mentioned for $L=\infty$ are linear extrapolations in $1/L$.

L'	L	$N(L;0)$	$N(L;1)$	$\bar{d}(L', L; 0)$	$\bar{d}(L', L; 1)$
	2	3.5	2.8922541		
2	3	7.6165	5.3723743	1.91768	1.527 22
3	4	13.070 (5)	8.370 (3)	1.877 (1)	1.541 (1)
4	5	20.016 (7)	11.863 (5)	1.910 (3)	1.563 (3)
5	6	28.47 (1)	15.99 (5)	1.932 (4)	1.572 (4)
6	7	38.55 (1)	20.198 (7)	1.966 (4)	1.594 (5)
7	8	50.16 (1)	25.04 (1)	1.972 (4)	1.608 (6)
8	9	63.42 (2)	30.30 (1)	1.991 (4)	1.62 (1)
9	10	78.11 (2)	35.99 (1)	1.977 (6)	1.63 (1)
10	11	94.70 (2)	42.08 (2)	2.021 (5)	1.64 (1)
11	12	112.67 (3)	48.58 (5)	1.997 (6)	1.65 (2)
	∞			2.04 (2)	1.72 (4)

Carlo runs into, e.g., 10 groups of 10 000 runs each. If the partial results from these groups show a variance σ, the expected error on the total average is $\sigma/\sqrt{10}$. The extrapolations of $\bar{d}$ in terms of $1/L$ should be compared with the results obtained by Evertsz on large cylindrical cells [18]. Due to the fact that the DBM clusters are not self-similar but self-affine, our values for $\bar{d}$ do not coincide with the box-counting dimension D (1.663 ± 0.002 for $\eta = 1$), but they are compatible with the values for $1 + 1/\nu$, where ν is the scaling exponent for the average height h in terms of N: $h \sim N^{\nu}$.

For the same cylindrical cells we have also calculated the average moments M_q of the probabilities of all growth sites at breakdown, defined as

$$M_q = \sum_i P_i^q \qquad \text{where } P_i = \Delta\Phi_i^{\eta} / \sum_j \Delta\Phi_j^{\eta}. \tag{3.2}$$

These M_q are known to scale like

$$\frac{M_q(L)}{M_q(L')} \simeq \left(\frac{L}{L'}\right)^{-(q-1)D(q)} \tag{3.3}$$

where $D(q)$ is the multifractal dimension [19].

For negative q values the moments are dominated by the sites with the smallest growth probabilities. If extremely small growth probabilities can be found in configurations with a very small weight factor, they may be very hard to discover by standard Monte Carlo procedures. We have therefore performed the following test to see whether the MC moment calculations can be trusted. On cylindrical $L \times L$ cells we calculated these moments through a set of 100 000 independent MC runs. The intermediate results were collected in three different ways: (a) in 1000 sets of 100 runs, (b) in 100 sets of 1000 runs and (c) in 10 sets of 10 000 runs. For each of these subdivisions, we calculated the variance of the average results in each set. If we call these variances respectively σ_{100}, σ_{1000} and $\sigma_{10\,000}$, we should expect that $\sigma_{100}/\sigma_{10\,000} = (\sigma_{100}/\sigma_{1000})^2 = 10$, at least if the results from different runs have a nice statistical distribution. The results of this test are reproduced in table 3. This table shows that, while the moments obtained for positive q show a good statistical distribution, those for $q < -1$ clearly do not have this property. Since the σ-ratio approaches 1 for large L values, this means that the accuracy of a Monte Carlo calculation for these quantities cannot be improved by using larger samples! Further evidence of the deficiency of these negative moment calculations may be obtained from the ratio between these variances and the average value of the moments over the sample of 100 000 runs, as shown in table 4. It is only for $q > -1$ that the variance becomes smaller than the average. Since these effects become more pronounced for larger L, this means that one should also seriously question the accuracy of previously derived results for negative q values through Monte

Table 3. Values obtained for $\sigma_{100}/\sigma_{10\,000}$ on the $L \times L$ cylindrical configuration, for the moments M_q.

q	$L=3$	$L=4$	$L=5$	$L=6$	$L=7$	$L=8$	$L=9$
−3	11.10	2.52	1.96	1.03	1.01	1.03	1.47
−2	11.11	3.88	3.22	1.27	1.12	1.14	2.08
−1	10.34	7.78	7.56	4.34	3.82	2.81	5.05
0	10.73	7.92	10.37	10.56	12.26	8.76	11.23
0.5	10.96	10.49	8.88	11.44	12.73	9.63	11.20
2	10.81	9.21	10.46	8.80	8.71	13.63	12.63

Table 4. Values obtained for σ_{100}/M_q on the $L \times L$ cylindrical configuration.

q	$L=3$	$L=4$	$L=5$	$L=6$	$L=7$	$L=8$	$L=9$
−3	0.29	2.67	2.88	2.99	2.97	3.00	2.87
−2	0.22	1.56	2.13	2.82	2.82	2.96	2.62
−1	0.13	0.25	0.39	0.71	0.80	1.33	1.09
0	0.031	0.027	0.024	0.020	0.020	0.018	0.018
0.5	0.011	0.0077	0.0062	0.0049	0.0045	0.0041	0.0037
2	0.0075	0.0047	0.0047	0.0050	0.0064	0.0070	0.0075

Carlo calculations on larger systems. Our calculations indicate that the estimates obtained for $D(q)$ with $q < -1$ do not converge to a finite value when L increases. This confirms the calculations by Lee and Stanley [20]. In any case, we omit further analysis of these q values, except for $q = -1$.

In table 5 we show the results obtained for $D(q)$ with $q \geqslant -1$ through finite size scaling (using L and L'). When plotted against $1/L$, these estimates fall nicely on a straight line, such that their extrapolations for $L \to \infty$ can easily be obtained. These extrapolations are also included in the table.

Multifractal properties are often expressed in terms of a function $f(\alpha)$ giving the fractal dimension of the set of points where the probabilities P_i, defined in (3.2), scale with an exponent α. An analysis along these lines reproduces qualitatively the left part of the $f(\alpha)$ curve as reproduced, e.g., by Nagatani [7] or by Hayakawa *et al* [17]; the other part of the curve corresponds to negative q values.

We have also applied our combined enumeration and Monte Carlo computation to square cells, in which the full boundary is fixed at $\Phi = 1$ and the centre site at $\Phi = 0$ as seed. For even L, there is no centre site in the strict sense, so we take one of the four sites nearest to the centre. We have collected some results in table 6. Due to the special situation for the even L, the scaling does not work well when an odd L is combined with an even L'; therefore we analysed only the even-even and odd-odd combinations. Even then we can see in the table that there are large even-odd fluctuations in the predictions. One possibility to remedy for these fluctuations is to

Table 5. Values obtained from FSS with cylindrical cells of length L and L' for the multifractal dimensions $D(q)$, related to the moments of the probability distribution at breakdown for $\eta = 1$. The values mentioned for $L = \infty$ are linear extrapolations in $1/L$.

L'	L	$D(-1)$	$D(0)$	$D(0.5)$	$D(1.5)$	$D(2)$	$D(3)$	$D(4)$	$D(5)$
2	3	2.871	1.613	1.308	1.09855	1.05013	0.98014	0.92999	0.892795
3	4	3.38 (1)	1.616 (3)	1.199 (2)	0.9671 (5)	0.9252 (5)	0.8663 (5)	0.822 (1)	0.788 (4)
4	5	3.68 (2)	1.588 (2)	1.145 (2)	0.8958 (6)	0.8488 (7)	0.7865 (4)	0.7431 (5)	0.7107 (8)
5	6	3.94 (3)	1.562 (2)	1.1145 (15)	0.8513 (6)	0.7981 (7)	0.7296 (5)	0.6852 (5)	0.6541 (7)
6	7	4.2 (2)	1.54 (1)	1.093 (5)	0.822 (2)	0.765 (2)	0.6925 (20)	0.648 (2)	0.618 (2)
7	8	4.0 (3)	1.54 (1)	1.086 (5)	0.798 (3)	0.734 (3)	0.656 (3)	0.611 (3)	0.581 (3)
8	9	6.3 (6)	1.53 (1)	1.074 (4)	0.775 (3)	0.706 (3)	0.625 (3)	0.578 (3)	0.552 (4)
9	10	5.0 (1.5)	1.536 (7)	1.063 (3)	0.766 (4)	0.698 (4)	0.618 (4)	0.572 (5)	0.541 (7)
10	11	6 (2)	1.550 (5)	1.056 (3)	0.748 (3)	0.678 (3)	0.595 (4)	0.550 (4)	0.521 (6)
	∞	5 (1)	1.47 (3)	1.005 (3)	0.63 (1)	0.53 (1)	0.45 (1)	0.38 (1)	0.36 (1)

Table 6. Same as in table 2, but for squares with full boundary at $\Phi = 1$ and starting in the centre. The values $\bar{d}'$ contain corrections for the fact that for even L it is impossible to start really in the centre of the square.

L'	L	$N(L;0)$	$N(L;1)$	$\bar{d}(L',L;0)$	$\bar{d}(L',L;1)$	$\bar{d}'(L',L;0)$	$\bar{d}'(L',L;1)$
	3	4.018	3.488				
	4	5.652	4.546				
3	5	9.473	7.287	1.679	1.442		
4	6	12.275	8.864	1.912	1.647	1.802	1.525
5	7	17.868	12.338	1.886	1.565		
6	8	22.006	14.390	2.029	1.684	1.968	1.612
7	9	29.588	18.677	2.007	1.650		
8	10	35.160	21.180	2.100	1.732	2.063	1.684

add 0.5 to all $N(L)$ for even L; the seed is indeed half a lattice distance removed from the real centre of the square. In table 6 we have included the values for $\bar{d}$ obtained in this way, and we called them $\bar{d}'(L', L; \eta)$. These values interpolate much better between the values obtained with odd L and L'.

From the tables it is clear that the convergence of the results from this second type of cells is much slower than that for the cylindrical cells. This may be understood from the anisotropies present in the square cells with seed site in the middle. Furthermore, the distance between the seed and the $\Phi = 1$ boundary is actually $L/2$ in the second type of cells, while it is L in the cylindrical cells. We have also performed some calculations on the moments M_q for this second type of cells. Again, the convergence is much worse than for the cylindrical cells, although the corresponding values for the dimensionalities $D(q)$ have the same order of magnitude.

The general conclusion from our tables is rather clear. They prove that it is indeed possible to obtain very good estimates on the fractal properties of the DBM through the finite size scaling method, without the need to perform Monte Carlo calculations on very large systems. Our relatively small systems do already give estimates for $\bar{d}$ that lie well within the nowadays accepted range of values. Convergence is remarkably better for the cells with cylindrical configuration. The values for the multifractal exponents D_q converge slower than those for the fractal dimensions, as could be expected. The estimates obtained for them, however, are in full qualitative agreement with the behaviour obtained for this function by Hayakawa *et al* [17] and they do not conform with the conjecture that $D(q) \leqslant 1$ [21]. We also conclude that it is very dangerous to estimate negative moments through Monte Carlo calculations; only the use of small cells allows us here to study the distribution of the estimates over such a large sample of runs.

Appendix. Construction of the resistivity matrix

In order to obtain an accurate and efficient method for calculating the electrostatic potential Φ on the sites of a resistor network, we need to invert the method proposed by Derrida *et al* [22] in which a matrix A is constructed relating the currents injected at lattice sites j to the resulting potentials at sites k by

$$I_j = \sum_k A_{jk} \Phi_k. \tag{A1}$$

Such a matrix A in itself is not very useful for our purpose; imposing that an internal site of the lattice has no current leads to the discrete Laplace equation expressing that Φ_j is the average of the Φ_i at the neighbouring sites i of j. This is the equation used in the relaxation method. What we need is an expression for Φ_j in terms of the I_k; we thus need the inverse of A.

Since a constant choice for Φ_k leads to zero currents, the matrix A is singular and does not have a straightforward inverse. This can be solved by choosing an arbitrary lattice site to be fixed at $\Phi = 0$. This site does not have to be included in our index set $\{j\}$; due to charge conservation its current will have to compensate ΣI_j. A natural choice for this site in the DBM simulations is the central seed for the cluster growth. From now on, we will call this site the seed site.

For the remaining sites in our system, we can now try to construct the matrix B defined by

$$\Phi_j = \sum_k B_{jk} I_k. \tag{A2}$$

The first problem is that we should never try to numerically calculate the matrix elements B_{ij} for sites belonging to disconnected parts of the lattice, since the corresponding B values, having the meaning of resistances, will be infinite. The following prescription is only computable for a fully interconnected set of sites. Furthermore, we should include the site indices one by one into our index set, while adding to our matrix the first contribution of the resistances which link these sites to the rest of the system.

The algorithm for constructing the resistivity matrix B consisting of three distinct parts, each to be repeated as many times as necessary.

1. The initial step is to include in the index set all sites directly connected through some resistances R_j to the seed (see figure 1). Since along these resistances we have a potential drop $\Phi_j = R_j I_j$ (if no other interconnecting resistances are present), we obviously have the starting rule for these sites:

$$B_{jj} = R_j. \tag{A3}$$

2. The addition of a new site i to an already treated configuration of sites will have to occur through a resistance link with value R between i and some site j of the configuration (see figure 2). This will change the matrix B into $\tilde{B}$ in the following way. The current I_i entering site i will flow into the system at site j, where it will be added to the current I_j. Thus, for all k (including j) we may write

$$\tilde{B}_{ki} = B_{kj}. \tag{A4}$$

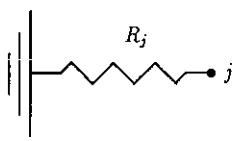

Figure 1. Inclusion of first site.

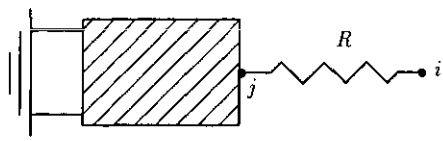

Figure 2. Addition of a new site.

Furthermore, since $\Phi_i = \Phi_j + I_i R$, we also have that

$$\tilde{B}_{ik} = B_{jk} \tag{A5}$$

$$\tilde{B}_{ii} = B_{jj} + R. \tag{A6}$$

3. The third operation that we must be able to describe is the addition of a resistance R betwen two sites i and j already belonging to the configuration. In order to keep the potentials Φ_k unchanged, the currents I_i and I_j should be changed into $\tilde{I}_i$ and $\tilde{I}_j$ as follows (see figure 3):

$$\tilde{I}_i = I_i + \frac{1}{R}(\Phi_i - \Phi_j) \tag{A7}$$

$$\tilde{I}_j = I_j + \frac{1}{R}(\Phi_j - \Phi_i) \tag{A8}$$

and we need to know how B transforms into $\tilde{B}$, with

$$\Phi_k = \sum_m B_{km} I_m = \sum_m \tilde{B}_{km} \tilde{I}_m. \tag{A9}$$

The result of a straightforward calculation is

$$\tilde{B}_{km} = B_{km} - \frac{(B_{ki} - B_{kj})(B_{mi} - B_{mj})}{R + B_{ii} + B_{jj} - 2B_{ij}} \tag{A10}$$

valid for all k and m (i and j included). This result is also valid for $R = 0$, i.e. for short-circuiting i and j.

We should add the following remarks:

(i) The matrix is symmetric: $B_{ij} = B_{ji}$. This can be used to save computation time or memory capacity.

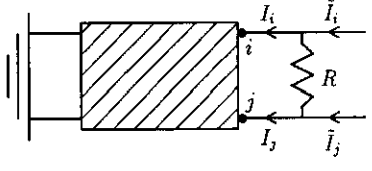

Figure 3. Addition of a new resistance.

(ii) If (as in the DBM) the only constraint is that a given site a (the boundary, for example) is kept at unit potential, the only current will be I_a, and thus for the voltage at a: $\Phi_a = 1 = B_{aa} I_a$. The potential at all other sites is then obtained from

$$\Phi_i = \frac{B_{ai}}{B_{aa}}. \tag{A11}$$

(iii) The net resistivity between sites i and j is given by

$$R_{ij} = B_{ii} + B_{jj} - 2B_{ij}. \tag{A12}$$

In combination with (A10) this leads to the complementary transformation rule

$$\tilde{R}_{km} = R_{km} - \frac{(R_{ki} - R_{kj} + R_{mi} - R_{mj})^2}{4(R + R_{ij})} \tag{A13}$$

for the operation described in figure 3.

(iv) Equation (A10) can in principle also be applied for $R < 0$. One might want to do this if an existing resistance R between i and j should be deleted, which can be achieved by adding a fictional resistance $(-R)$ in parallel between the same sites. This may, however, lead to infinite matrix elements when a site becomes in this way disconnected from the network.

(v) If one is not really interested in what happens in a subset of the lattice sites (where the currents must be zero), one may drop these sites from the calculation, once all their links with the rest have been realized. While adding the last resistance to a site, its index can, e.g., be re-used for the newly added lattice site; equations (A4) and (A5) are then automatically satisfied. Such a procedure, which can lead to an enormous reduction of computer savings, leads to the strip transfer method as used by Derrida *et al* [22].

References

[1] Niemeyer L, Pietronero L and Wiesmann H J 1984 *Phys. Rev. Lett.* **52** 1033
[2] Witten T A and Sander M 1981 *Phys. Rev. Lett.* **47** 1400
[3] Meakin P 1988 *Phase Transitions and Critical Phenomena* vol 12, ed C Domb and J L Lebowitz (New York: Academic) p 336
[4] Gould H, Family F and Stanley H E 1983 *Phys. Rev. Lett.* **50** 686
[5] Nakanishi H and Family F 1985 *Phys. Rev.* A **32** 3606
[6] Nagatani T 1987 *J. Phys. A: Math. Gen.* **20** L381; 1987 *Phys. Rev.* **36** 5812
[7] Nagatani T 1988 *J. Phys. A: Math. Gen.* **21** L655
[8] Wang X R, Shapir Y and Rubinstein M 1989 *J. Phys. A: Math. Gen.* **22** L507
[9] Wang X R, Shapir Y and Rubinstein M 1989 *Phys. Rev.* A **39** 5974
[10] Pietronero L, Erzan A and Evertsz C 1988 *Phys. Rev. Lett.* **61** 861; 1988 *Physica* A **151** 207
[11] Nightingale P 1983 *J. Appl. Phys.* **53** 7927
Barber M N 1983 *Phase Transitions and Critical Phenomena* vol 8, ed C Domb and J L Lebowitz (New York: Academic) p 145
[12] Dhar D 1985 *Phys. Rev. Lett.* **54** 2058
[13] Ball R C and Witten T A 1984 *Phys. Rev.* A **29** 2966
[14] Muthukumar M 1983 *Phys. Rev. Lett.* **50** 839
[15] Matsushita M, Honda K, Toyoki H, Hayakawa Y and Kondo H 1986 *J. Phys. Soc. Japan* **55** 2618
[16] Martin J L 1974 *Phase Transitions and Critical Phenomena* vol 3, ed C Domb and M S Green (New York: Academic) p 97
[17] Hayakawa Y, Sato S and Matsushita M 1987 *Phys. Rev.* A **36** 1963
[18] Evertsz C 1990 *Phys. Rev.* A **41** 1830
[19] Hentschel H G E and Procaccia I 1983 *Physica* **8D** 435
[20] Lee L and Stanley H E 1988 *Phys. Rev. Lett.* **61** 2945
[21] Halsey T C, Meakin P and Procaccia I 1986 *Phys. Rev. Lett.* **56** 854
[22] Derrida B, Zabolitsky J G, Vannimenus J and Stauffer D J 1984 *J. Stat. Phys.* **36** 31